Korean J. Chem. Eng., 37(9), 1482-1489 (2020)
DOI: 10.1007/s11814-020-0557-7

pISSN: 0256-1115
eISSN: 1975-7220

Kinetic study on the reaction of palmitic acid with ethanol catalyzed by deep eutectic solvent based on dodecyl trimethyl ammonium chloride

Shan Jiang, Zuoxiang Zeng[†], Weilan Xue, Wei Zhang, and Zhiyuan Zhou

Institute of Chemical Engineering, East China University of Science and Technology, 200237 Shanghai, China

(*Received 5 December 2019 • Revised 22 March 2020 • Accepted 12 April 2020*)

Abstract−This study explored the direct esterification of palmitic acid and ethanol using a deep eutectic solvent (DES) as catalyst to produce biodiesel. Three novel deep eutectic solvents (DTAC-PTSA, DTAC-2PTSA, DTAC-3PTSA) were successfully prepared by mixing dodecyl trimethyl ammonium chloride (DTAC) and p-toluenesulfonic acid monohydrate (PTSA) in a molar ratio of 1: *z* (*z*=1, 2, 3). After testing, DTAC-3PTSA was found to have the best catalytic performance among the three types of DESs and was therefore selected as the catalyst for subsequent experiments. The effects of agitation speed, ethanol to palmitic acid molar ratio (α), temperature and catalyst dosage were studied by investigating the change of palmitic acid conversion rate with time under different conditions, respectively. Then, the pseudo-homogeneous (PH) model was utilized to describe the kinetic behavior of this reaction between 328.15-348.15 K and it was found to work well for the experimental data obtained. Moreover, the catalytic performance of DTAC-3PTSA was detected to have no significant change in the cycle test. Therefore, DTAC-3PTSA can be considered as a substitute for traditional catalysts to produce biodiesel and the kinetic data obtained here can be used for further up-scaling study.

Keywords: Deep Eutectic Solvent, Biodiesel, Ethyl Palmitate, Esterification, Kinetics

INTRODUCTION

Ethyl palmitate is an important portion of biodiesel [1-3] that has been studied intensively with the aim of developing a new generation of renewable and economically sustainable energy sources. Biodiesel is generally made from vegetable oil or animal fat and can be directly applied to diesel engines, replacing fossil fuels. This biofuel is commonly made in two routes [4-7]: transesterification, in which glycerol is generated as byproduct and it must be separated from the target product, and the second one is the esterification reaction between the fatty acids and alcohol (methanol or ethanol). For the second method, liquid acids (such as H_2SO_4) are generally used as catalysts for esterification reactions [8]. Even so, these catalysts have some severe defects of equipment corrosion, large excess of alcohol, tough recycle ability and huge wastewater amount.

To overcome these disadvantages, several novel catalysts (ionic liquids [9,10], solid acids [11,12], ion exchange resins [13], deep eutectic solvents (DESs) [14] and novel carbon-based materials [15, 16]) have been proposed. In recent decades, DES has gained wide attention and found to have a bright future in biodiesel production due to the strengths of non-flammability, non-toxicity, easy separation and reusability [17,18]. DES is a mixture of HBD (hydrogen bond donor, such as carboxylic acids, metal halides, amines and a member of alcohols) and HBA (hydrogen bond acceptor, such as quaternary ammonium salts). Compared to its components, DESs have been detected to have a lower melting point. Therefore, DESs have been extensively studied as a promising solvent [19] or liquid catalyst [20] (especially in liquid reactions) in recent decades. Cao et al. achieved a high-efficiency esterification reaction of formic acid or acetic acid with alcohol using a deep eutectic solvent (choline chloride/chromium chloride hexahydrate) as catalyst [21]. Lee et al. synthesized methyl palmitate with DESs as solvent-catalyst and optimized the conditions of reaction [22]. Tran et al. developed a new and efficient method for the arylation of benzoxazole with aromatic aldehydes under the catalysis of deep eutectic solvents [23]. Gu et al. synthesized a new type of deep eutectic solvent as a homogeneous reaction catalyst to prepare biodiesel [24].

In the open literature, there are few experimental data on the dynamics of the esterification of ethanol and palmitic acid. Therefore, it is necessary to explore the dynamics of this reaction, and the kinetic data obtained would be beneficial for the process design and simulation. The esterification reaction equation of ethanol and palmitic acid can be seen in Scheme 1, where A, B, C, and D refer to palmitic acid, ethanol, ethyl palmitate and water, respectively.

In this paper, three novel DESs based on dodecyl trimethyl ammonium chloride (DTAC-*z*PTSA; *z*=1, 2, 3 means the number of moles of PTSA relative to per 1 mole of DTAC) were successfully synthesized and tested. It was found that DTAC-3PTSA has the best catalytic performance among the three deep eutectic solvents, and DTAC-3PTSA was therefore selected as the catalyst for subsequent experiments. The reaction kinetics on esterification of ethanol with palmitic acid using DTAC-3PTSA as catalyst was studied during the temperature of 328.15-348.15 K. After that, the influence of operating parameters on the conversion of palmitic acid was considered, including agitation speed, initial molar ratio of ethanol to palmitic acid ($\alpha=(n_{ethanol}/n_{acid})_{initially}$, the following is the same), reac-

---

[†]To whom correspondence should be addressed.
E-mail: zengzx@ecust.edu.cn

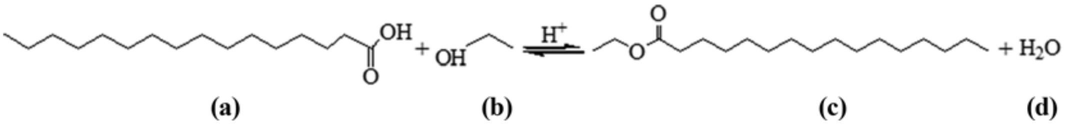

Scheme 1. Esterification reaction equation of palmitic acid and ethanol.

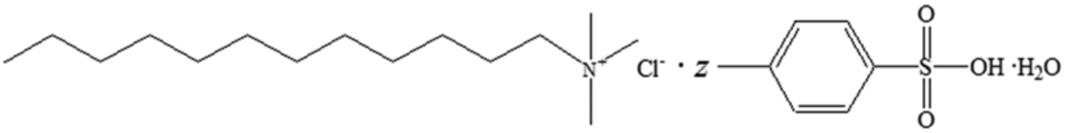

Scheme 2. Chemical formula of DTAC-*z*PTSA.

tion temperature and catalyst dosage. Ultimately, a pseudo-homogeneous (PH) model was developed to correlate the experimental kinetic data [25].

EXPERIMENT

1. Materials

Dodecyl trimethyl ammonium chloride (purity ≥99%) was supplied by Titan Scientific Co. Ltd., Shanghai, China; p-toluenesulfonic acid monohydrate (purity ≥99%) was obtained from Di Bo Chemical Co. Ltd.; palmitic acid (purity 97%) was supplied by Acmec Biochemical Co. Ltd., Shanghai, China; ethanol (purity 99.5%) was purchased from Titan Scientific Co. Ltd., Nanjing, China.

2. Preparation of DESs

DESs in this work were synthesized by mixing DTAC and PTSA in a molar ratio of 1: *z* (*z*=1, 2, 3). Its chemical composition is shown

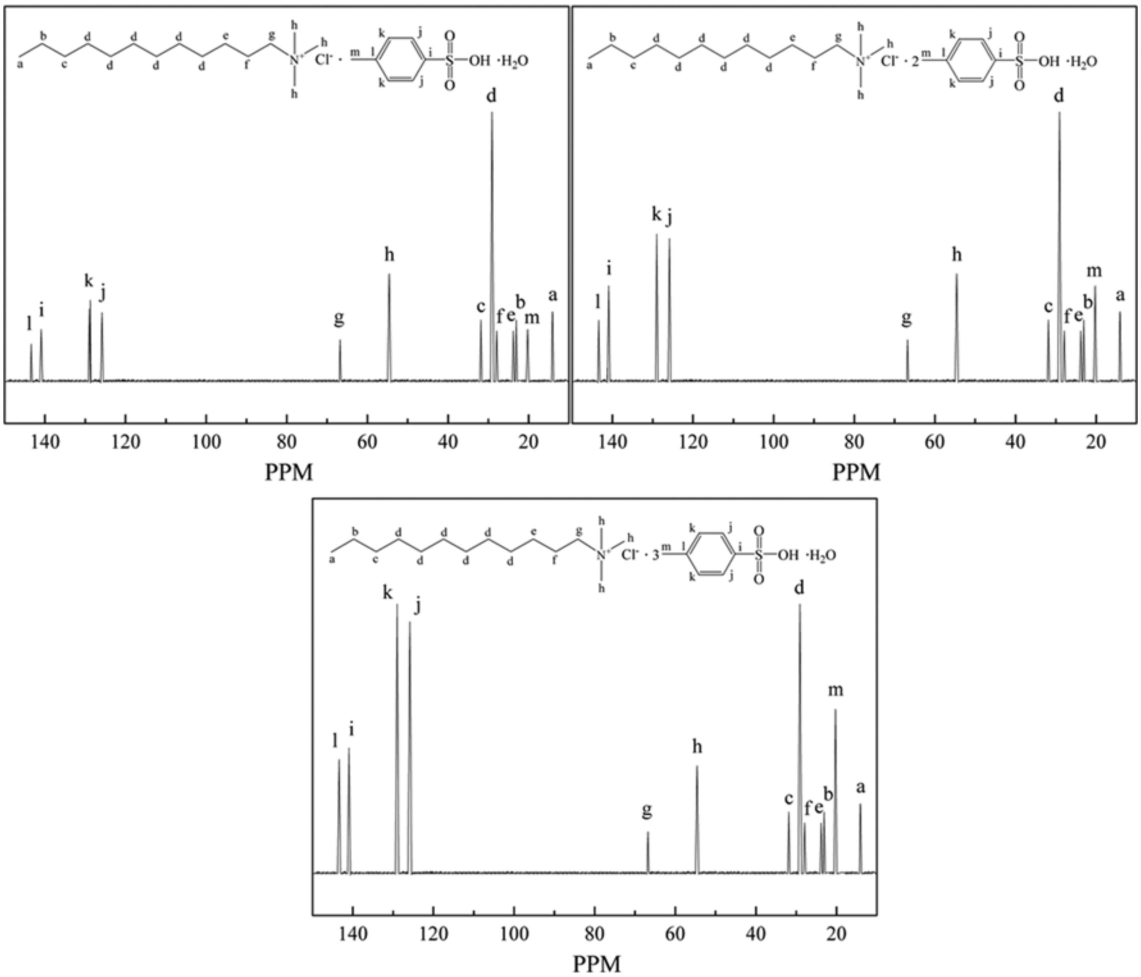

Fig. 1. ^{13}C-NMR spectrum of DTAC-*z*PTSA (z=1, 2, 3).

Table 1. Physical properties and composition of the DTAC-*z*PTSA (z=1, 2, 3)

DESs	Feed molar ratio (DTAC/PTSA)[a]	Practical molar ratio (DTAC/PTSA)[b]	pH[c]	Freezing point
DTAC-PTSA	1 : 1	1 : 1.03	1.98	307.15 K
DTAC-2PTSA	1 : 2	1 : 1.95	1.05	283.65 K
DTAC-3PTSA	1 : 3	1 : 2.96	0.28	317.15 K

[a] The molar ratio of DTAC to PTSA used to prepare DES.

[b] The molar ratio of DTAC to PTSA tested by ^{13}C-NMR spectrometer.

[c] The pH of DTAC 10% aqueous solution: 6.89; the pH of PTSA 10% aqueous solution: 0.28.

in Scheme 2. The DTAC-*z*PTSA was prepared as follows: A quantity of p-toluenesulfonic acid monohydrate and dodecyl trimethyl ammonium chloride was dried under vacuum at 338.15 K for 1 hour, and then mixed together at 348.15 K for 1 hour with constant stirring until a light yellow homogeneous liquid formed. After the mixture was cooled to 25 °C and became solid, it was sealed and stored in a desiccator for the next use.

3. Characterization of DESs

The ^{13}C-NMR spectrometer [26] (Bruker Advance 400 MHz) was used to investigate the chemical composition of DTAC-*z*PTSA (z=1, 2, 3) with a solution of $CDCl_3$. The obtained ^{13}C-NMR spectrum is shown in Fig. 1. The positions of the characteristic peaks of the three DESs are almost the same. From Fig. 1, it can be found that several characteristic peaks appear at 14.1 (a), 23.1 (b), 31.8 (c), 29.1 (d), 23.8 (e), 27.9 (f), 66.8 (g) and 54.6 (h), corresponding to carbons of the long carbon chain and the carbons attached to atom N in DTAC, respectively. The characteristic peaks at 140.9 (i), 125.9 (j), 129.0 (k), 143.4 (l) and 20.3 (m), respectively, refer to carbons of benzene ring and carbon in methyl group in PTSA. The relative content of DTAC and PTSA in the DTAC-*z*PTSA can be obtained by calculating the peak areas at 14.1 (a) and 20.3 (m), the results of which are consistent with the actual feed molar ratio (Table 1). The freezing point and pH value of DTAC-*z*PTSA were measured as shown in Table 1.

The Fourier transform infrared (FTIR) spectrometer (Nicolet MQGNA-IR 550) was utilized to detect the functional groups of DTAC, PTSA and DTAC-*z*PTSA. By comparing the spectra in Fig. 2, the absorption spectra of the three kinds of DESs are almost the same and contain similar absorption peaks as DTAC and PTSA. In the DESs spectrum, the peaks appearing at 1,260-1,000 cm^{-1} and 1,000-910 cm^{-1} indicate the presence of S=O and C-N, respectively. In addition, there are characteristic absorptions of long carbon chains, that is, the deformation absorption of CH_2 at 800-750 cm^{-1} and the absorption of CH_3 at 1,500-1,377 cm^{-1}.

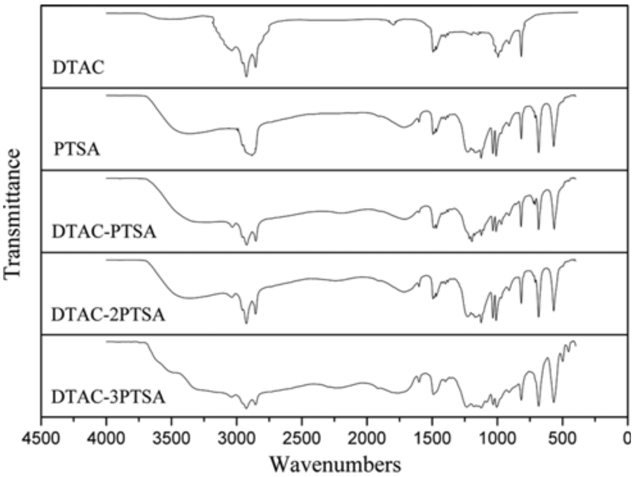

Fig. 2. FTIR spectrum of DTAC, PTSA and DTAC-*z*PTSA (z=1, 2, 3).

4. Esterification Reaction

Esterification reaction was performed in a 250 mL dry four-neck flask equipped with reflux condenser, sampling port, a mercurial thermometer and a stirrer. The reaction temperature was kept constant by using the constant temperature water bath. First, the weighed ethanol and palmitic acid were placed in the reactor and heating was started; second, the weighed catalyst was added when the reactor temperature reached the required value, and timing was begun; and third, samples were taken at specific intervals and placed quietly at room temperature for 30 seconds to prevent further reactions, then they were tested by gas chromatography (GC) [27]. GC was conducted on Shimadzu GC-2014C equipped with a SE-30 capillary column (30 m×0.32 mm i.d. ×0.5 μm in thick), nitrogen was utilized as carrier gas, the inlet temperature and the temperature of hydrogen flame ionization detector (FID) was 553.15 K and 573.15 K, respectively.

5. Selection of DESs

In this study, three kinds of DESs (DTAC-PTSA, DTAC-2PTSA, DTAC-3PTSA), pure DTAC and pure PTSA were utilized as catalysts in the esterification reaction, respectively. The experiments were conducted under the conditions of 0.6 mol ethanol, 0.2 mol palmitic acid (α=3), 4.74 g catalyst (6% w/w, based on the mass of all reactants, the following is similar), temperature of 348.15 K and rotation speed of 600 rpm. Samples were taken at 30 minutes, 60 minutes and 180 minutes from the start of the reaction. The GC was used to obtain the sample composition. The experimental results are shown in Table 2. It was found that the catalytic activity of DTAC is poor while PTSA exhibits good catalytic activity, similar to DESs. Therefore, it could be inferred that the high reaction rate of esterification is mainly attributed to the acidic active sites provided by PTSA in DESs. Comparing the experimental results with three kinds of DESs as catalysts, the obtained palmitic acid conversion rate was the highest when the DTAC-3PTSA was used as catalyst. Furthermore, DTAC-3PTSA has the unique advantage of easy separation compared to conventional acidic catalysts. Therefore, DTAC-3PTSA was selected as the catalyst for subsequent experiments.

Table 2. The palmitic acid conversion of the samples with different catalysts

Catalyst	Conversion of palmitic acid[a] (%)		
	30 min	60 min	180 min
DTAC-PTSA	63.2	74.8	85.2
DTAC-2PTSA	68.3	78.5	86.9
DTAC-3PTSA	71.9	80.8	87.8
PTSA	74.5	83.2	88.5
DTAC	4.5	7.3	14.5

[a] Reaction conditions: 348.15 K; 600 rpm; α=3 and 6% w/w catalyst.

6. The Experiments of Kinetic and Chemical Equilibrium

One of the dynamics experiments was taken as an example: First, 0.6 mol of ethanol and 0.2 mol of palmitic acid (α=3) were placed in the reactor, then heating was started; second, 6% w/w DTAC-3PTSA was added when the reactor temperature reached the required value, and timing was begun; third, samples were taken at specific intervals and placed quietly at room temperature for 30 seconds to prevent further reactions, then they were tested by GC.

A chemical equilibration experiment [28] was run at four different temperatures (328.15 K, 335.15 K, 342.15 K, 348.15 K) using almost the same experimental procedure as the kinetic experiment (under the conditions of 0.2 mol of palmitic acid, 0.6 mol of ethanol, 6% w/w of DTAC-3PTSA and a rotation speed of 600 rpm). The samples were continuously taken out of the reaction system and analyzed until the composition of the mixture remained constant (sampling at 8 hours, 12 hours and 16 hours from the start of the reaction in this work). Some thermodynamic data for this reaction can be obtained by calculating the measured equilibrium data.

RESULTS AND DISCUSSION

1. Influence of Rotational Speed

The influence of rotational speed on the conversion of palmitic acid was investigated ranging from 200 rpm to 800 rpm at α=3 with a catalyst dose of 6% w/w, a temperature of 348.15 K and reaction time of 3 hours. From Fig. 3, the palmitic acid conversion rate increases as the rotational speed increases from 200 rpm to 600 rpm, while the palmitic acid conversion rate remains substantially unchanged in the range of 600 rpm to 800 rpm. The reason for this behavior may be that increasing the rotational speed in the range of 200 rpm to 600 rpm is conducive to promoting mass transfer and reducing the external diffusion resistance, while the external diffusion resistance substantially disappears when the rotational speed exceeds 600 rpm. Therefore, the subsequent experiments were conducted at 600 rpm.

2. Influence of Ethanol to Palmitic Acid Molar Ratio

The influence of initial ethanol to palmitic acid molar ratio was investigated by varying the α value from 1 to 3 under the condition of 348.15 K, catalyst dose of 6% w/w and reaction time of 3 hours. The results are shown in Fig. 4. It could be that the palmitic acid conversion rate will increase significantly as the proportion of ethanol increases. This might be because the esterification reaction is reversible and excess ethanol would drive the reaction forward.

3. Influence of Temperature

The influence of temperature on the palmitic acid conversion was investigated in the range of 328.15-348.15 K while the other reaction conditions were fixed at α=3, 6% (w/w) of catalyst dosage and 3 hours of reaction time. By comparing the shapes of four curves in Fig. 5, increasing the temperature can simultaneously improve the palmitic acid conversion rate and reaction rate. The reason might be that the chances of effective collision of reactant molecules would increase significantly at higher temperatures. That is, as the temperature increases, the number of old bonds breaks, and new bond formation per unit time also increases, which is manifested at the macro level as the reaction rate is accelerated.

4. Influence of Catalyst Dose

The influence of DTAC-3PTSA dose on the palmitic acid conversion was studied by varying the amount of catalyst from 2% w/w to 6% w/w while the other reaction conditions were fixed at α=

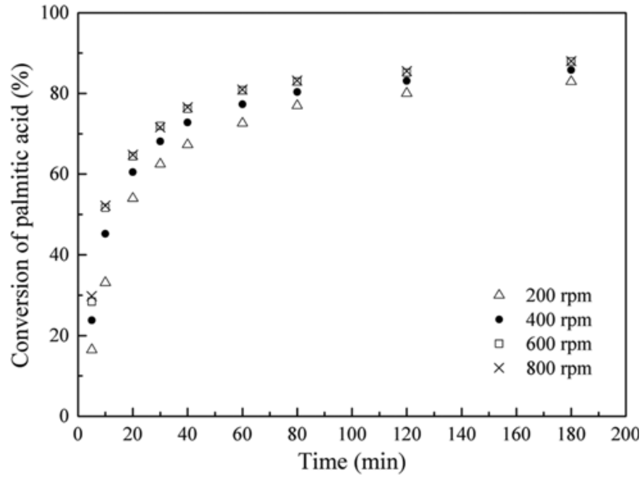

Fig. 3. The influence of agitation speed on the palmitic acid conversion (Temperature: 348.15 K; ethanol-acid molar ratio: 3; catalyst dosage: 6% w/w).

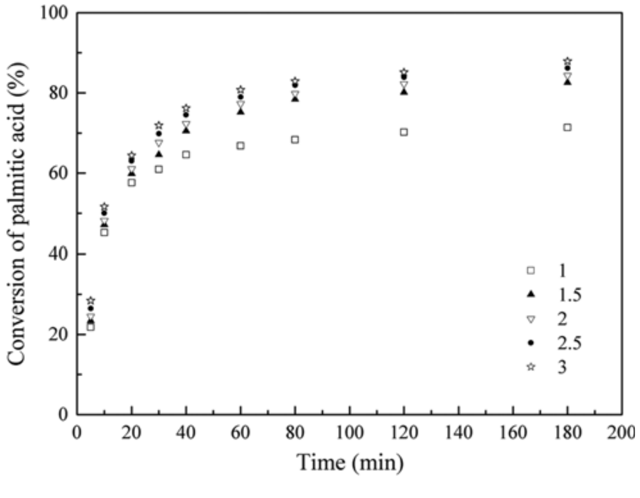

Fig. 4. The influence of ethanol-acid molar ratio (α) on the palmitic acid conversion (Catalyst dosage: 6% w/w; temperature: 348.15 K; agitation speed: 600 rpm).

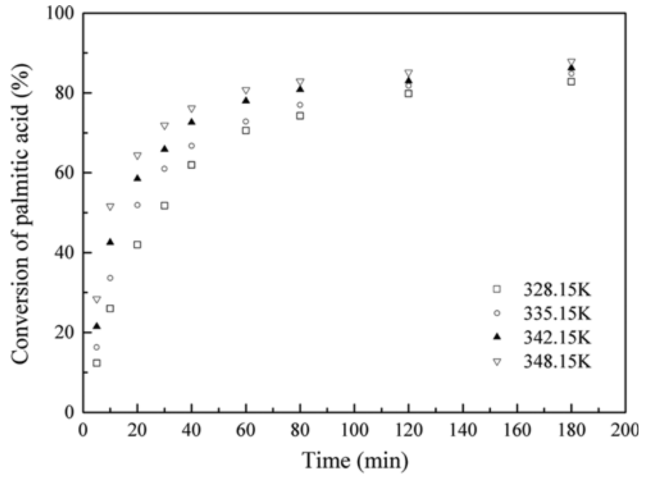

Fig. 5. The influence of temperature on the palmitic acid conversion (Ethanol-acid molar ratio: 3; catalyst dosage: 6% w/w; agitation speed: 600 rpm).

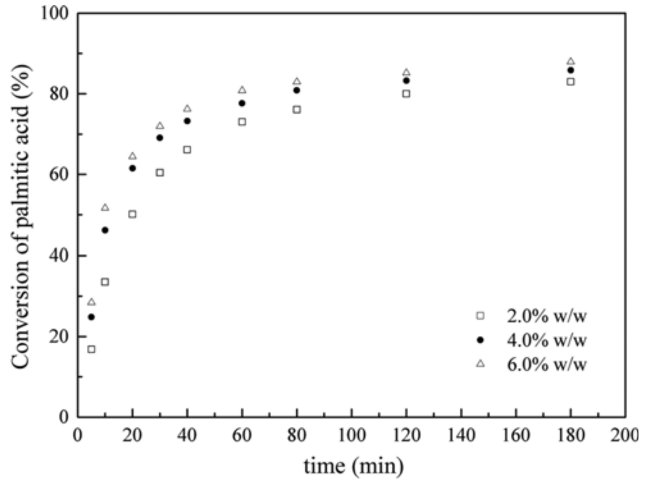

Fig. 6. The influence of catalyst dosage on the palmitic acid conversion (Agitation speed: 600 rpm; temperature: 348.15 K; ethanol-acid molar ratio: 3).

3, 348.15 K of temperature and 3 hours of reaction time. The experimental results are shown in Fig. 6. It is obvious that increasing the catalyst dosage is helpful to increase reaction rate. It can be explained that the higher the amount of catalyst used, the more the acidic active sites, which is beneficial for the reaction process. Furthermore, it was found that the reaction system gradually changed from clear to turbid in the course of the reaction. This might be because the hydrophilic DES is miscible with the reactants while immiscible with the produced ester. So, this transformation will occur when the mole fraction of produced ester reaches a specific amount to form the inverse emulsion (turbid). The esterification reaction takes place on the surface of the liquid globule of the inverse emulsion. Therefore, increasing the catalyst loading can increase the number of interphase reactions per unit volume, which speeds up the reaction.

5. Chemical Equilibrium

Chemical equilibrium constants can be obtained by calculating the equilibrium mole fraction of each component at four different temperatures (328.15 K, 335.15 K, 342.15 K, 348.15 K). Taking into account the deviation of the mixture solution from the ideal solution, the activity of each component was used to substitute the mole fraction in the calculation. The chemical equilibrium constants can be calculated experimentally by the following equation:

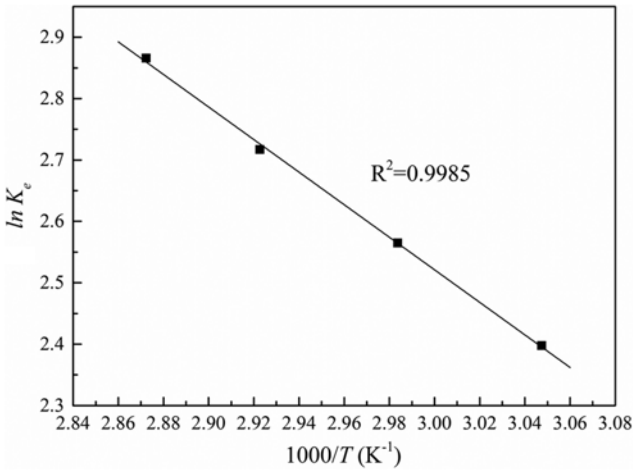

Fig. 7. The dependence of equilibrium constants on temperature.

$$K_e=\left(\frac{a_{ester}a_{H_2O}}{a_{acid}a_{E_tOH}}\right)_{eq}=\left(\frac{x_{ester}x_{H_2O}}{x_{acid}x_{E_tOH}}\right)_{eq}\bullet\left(\frac{\gamma_{ester}\gamma_{H_2O}}{\gamma_{acid}\gamma_{E_tOH}}\right)_{eq} \quad (1)$$

where K_e is chemical equilibrium constant, a_i indicates the activity of each component, x_i represents the mole fraction of each component, γ_i refers to the activity coefficient of each component. The activity coefficient was calculated by the UNIFAC model established by Fredenslund and Prausnitz et al. [29,30]. In this method, the activity coefficient is composed of a combination activity coefficient and a residual activity coefficient. The group area parameter, the volume parameter and the group interaction parameter to be used for calculation can be obtained from the reference [31].

The dependence of the calculated K_e on temperature is shown in Fig. 7. It was observed that $\ln K_e$ is linear with 1/T, and the mathematical expression is as follows:

$$\ln K_e=10.474-\frac{2.651\times10^3}{T} \quad (2)$$

The reaction entropy ($\Delta_r S^0$) and enthalpy ($\Delta_r H^0$) can be calculated by the following formula:

$$\ln K_e=\frac{\Delta_r S^0}{R}+\frac{-\Delta_r H^0}{RT} \quad (3)$$

The calculated values of $\Delta_r H^0$ and $\Delta_r S^0$ are 22.040 kJ mol^{-1} and 87.081 J mol^{-1} K^{-1}, respectively (by comparing Eq. (2) and Eq. (3)). The Gibbs free energy ($\Delta_r G^0$) of the reaction can be calculated by the following formula:

$$\Delta_r G^0=\Delta_r H^0-T\Delta_r S^0 \quad (4)$$

The value of $\Delta_r G^0$ (298.15 K) can be calculated to be −3.923 kJ mol^{-1}, which indicates that the reaction is spontaneous in the standard state.

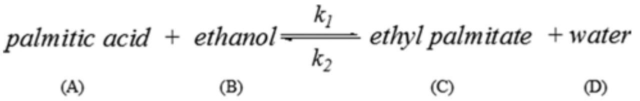

Scheme 3. Reaction of ethanol and palmitic acid to prepare ethyl palmitate.

6. Kinetic Modeling

The reaction equation for the reaction of palmitic acid with ethanol to prepare ethyl palmitate is as follows (Scheme 3):

The catalyst DTAC-3PTSA, the reactants and the products are both liquid at the reaction temperature. The effects of internal and external mass transfer resistance are almost negligible with sufficient agitation. This suggests that the kinetic behavior of the reaction can be investigated similarly to the homogeneous reaction. Therefore, a pseudo-homogeneous model was utilized to describe the kinetic behavior of this reaction in this work. The kinetic equation of the reaction rate based on the PH model can be written as Eq. (5) below:

$$r=\frac{1}{v_i}\frac{dn_i}{dt}=M_{cat}(k_1a_Aa_B-k_2a_Ca_D)=M_{cat}k_1\left(a_Aa_B-\frac{1}{K_e}a_Ca_D\right) \quad (5)$$

where r represents the reaction rate (mol min^{-1}); v_i represents the stoichiometric coefficient while n_i refers to the number of moles of component *i* (mol); k_1 and k_2 represent the forward and reverse reaction rate constants (mol min^{-1}); t is the time (min); M_{cat} represents the percentage of catalyst used in the mass of all reactants; a_A, a_B, a_C and a_D represent the activity of palmitic acid, ethanol, ethyl palmitate and water, respectively. The reaction rate was calculated by the Simpson integration in this work. Minimizing the sum of residual squares (SRS) of the experimental and calculated values was determined as the objective function, and the nonlinear least squares method was utilized to fit and optimize the kinetic parameters of the pseudo-homogeneous model. The objective function was expressed as:

$$SRS=\sum_{samples}(r_{exp}-r_{cal})^2 \quad (6)$$

where r_{exp} and r_{cal} represent the experimental and calculated values of the reaction rate, respectively. The kinetic parameters correlated by the above method are listed in Table 3.

The palmitic acid conversion between the experimental values and the calculated ones based on the PH model are compared in Fig. 8. It can be found that the relative deviation of experimental data and calculated data is substantially less than 5.0%. This also confirms that the PH model could describe the kinetic behavior of the reaction system well.

Table 3. The reaction rate constants in the PH model

T (K)	k_1 (mol min^{-1})	k_2 (mol min^{-1})	SRS
328.15	0.3883±0.0167	0.0353±0.0015	1.7×10^{-7}
335.15	0.5183±0.0583	0.0399±0.0044	1.8×10^{-6}
342.15	0.7050±0.0750	0.0466±0.0046	2.6×10^{-6}
348.15	0.9233±0.1316	0.0526±0.0073	6.9×10^{-6}

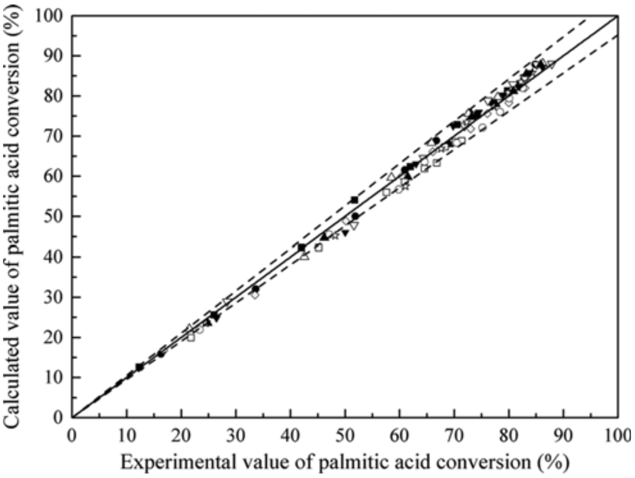

Fig. 8. The comparison of palmitic acid conversion between the experimental values and the calculated values based on the PH model (Temperature: (■) 328.15 K, (●) 335.15 K, (△) 342.15 K, (▽) 348.15 K; catalyst dosage: (◇) 2% w/w, (▲) 4% w/w, (▽) 6% w/w; the value of α: (□) 1, (○) 1.5, (☆) 2, (▼) 2.5, (▽) 3; (···) the deviation limits of ±5.0%).

Furthermore, the relationship between reaction rate and temperature could be obtained by Arrhenius equation [32], which is expressed as:

$$k_i=A_ie^{-Ea_i/RT} \text{ or } \ln k_i=\ln A_i-\frac{Ea_i}{RT} \quad (i=1,2) \quad (7)$$

where Ea_i and A_i represent activation energy and pre-exponential factor, respectively. The values of A_i and Ea_i were calculated by linearly regressing the relationship between $\ln k_i$ and 1/T; seeing Fig. 9, the mathematical expression of the reaction rate constant versus temperature is as follows:

$$k_1=1.36\times10^6\exp(-4948.4/T) \quad (8)$$

$$k_2=37.88\exp(-2293.0/T) \quad (9)$$

The values of the activation energy of the forward and reverse reaction are 41.141 kJ mol^{-1} and 19.064 kJ mol^{-1}, respectively. The kinetic data obtained above can be used in the design of industrial reac-

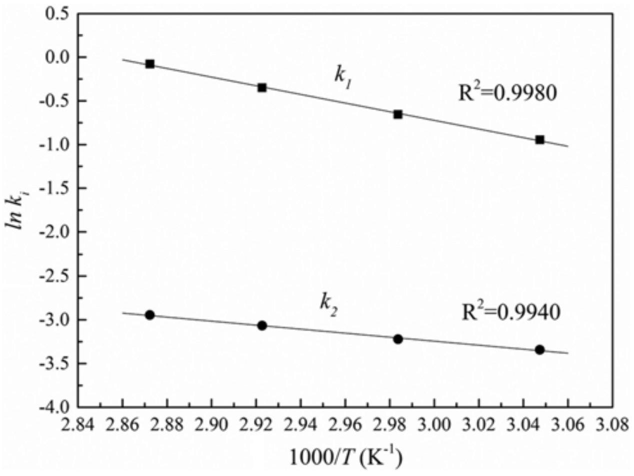

Fig. 9. The dependence of reaction rate constants on temperature.

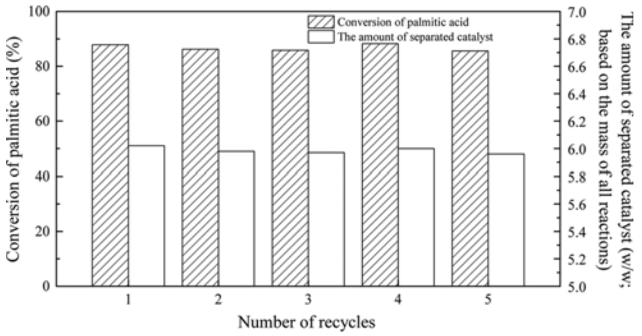

Fig. 10. The re-use performance of catalyst DTAC-3PTSA was detected through five cycles of testing.

tion equipment.

7. Recycling of DES

The separability and recyclability of catalysts are required by industrial application. Therefore, DTAC-3PTSA was separated in this work and its catalytic performance in cyclic tests was compared. After the reaction (reaction conditions: 348.15 K; 600 rpm; α=3 and 6% w/w catalyst), the reaction system was found to be gradually divided into an oil phase (above: ester) and an aqueous phase (below: water and DTAC-3PTSA). The water phase was separated by centrifugation, and then the water in the DTAC-3PTSA was removed via rotary evaporation. The separated catalyst would be further purified by vacuum drying at 338.15 K for 1 hour. Finally, five rounds of the same esterification reaction were studied with using the last separated DTAC-3PTSA. The conversion rate of palmitic acid and the amounts of separated catalysts after each reaction are shown in Fig. 10, and the experimental results reveal that there is no significant change in the reaction conversion rate and catalyst quality. Moreover, after each reaction, the pH values of the aqueous phase and the separated spent catalyst were detected, and the results obtained also indicated that the catalyst could be successfully recovered (the pH of aqueous phase: 0.52, 0.52, 0.53, 0.52, 0.52; the pH of separated catalyst: 0.28, 0.28, 0.28, 0.28, 0.29). Therefore, DTAC-3PTSA is more easily separated from the reaction system than the conventional homogeneous catalyst, and it still exhibits good catalytic performance in recycling.

CONCLUSIONS

Three novel deep eutectic solvents catalyst (DTAC-*z*PTSA) was successfully prepared by mixing dodecyl trimethyl ammonium chloride and p-toluenesulfonic acid monohydrate in a molar ratio of 1: *z* (*z*=1, 2, 3). After testing, it was found that DTAC-3PTSA had the best catalytic performance among the three deep eutectic solvents and was therefore selected as a catalyst for the esterification reaction. The effects of agitation speed, temperature, ethanol-acid molar ratio (α) and catalyst dosage were studied by investigating the change of palmitic acid conversion rate with time under different conditions. The results reveal that the DTAC-3PTSA exhibits good catalytic performance in the esterification reaction, and the palmitic acid conversion rate can reach more than 89% when the reaction conditions are fixed at α=3, 600 rpm of agitation speed, 348.15 K of temperature and 6% (w/w) of catalyst dosage. In this work, the pseudo-homogeneous model (PH) was used to describe the dynamics behavior and the two reaction rate constants were correlated (k_i). Based on the Arrhenius equation, the activation energies of the forward reaction and reverse reaction of the esterification reaction were also obtained (E_{a1}=41.141 kJ mol^{-1}, E_{a2}=19.064 kJ mol^{-1}). Moreover, the catalyst was detected to have excellent reuse performance through five cycles of testing. Therefore, DTAC-3PTSA can be considered as a substitute for traditional catalysts to produce biodiesel, and the kinetic data obtained here can be used for further scale up study.

NOMENCLATURE

K_e : equilibrium constant
a_i : activity of component *i*
r_i : reaction rate [mol min^{-1}]
M_{cat} : catalyst dosage [kg/kg]
γ_i : activity coefficient of component *i*
k_i : reaction rate constant [mol min^{-1}]
x_i : mole fraction of component *i*
SRS : minimum sum of residual squares
α : initial molar ratio of ethanol to palmitic acid
T : Temperature [K]
Ea_i : activation energy [kJ mol^{-1}]
$\Delta_r G^0$: Gibbs free energy [kJ mol^{-1}]
$\Delta_r S^0$: reaction entropy [J mol^{-1} K^{-1}]
$\Delta_r H^0$: reaction enthalpy [kJ mol^{-1}]
DTAC : dodecyl trimethyl ammonium chloride
PTSA : p-toluenesulfonic acid monohydrate
z : the number of moles of PTSA relative to per 1 mole of DTAC
DES : deep eutectic solvent
R^2 : linear regression coefficient

REFERENCES

1. L. Rafael, C. L. Jon, D. Bipasa, C. Joy, M. C. Juan and A. R. Antonio, *Energy Environ. Sci.*, **3**, 1706 (2010).
2. S. A. Renata, S.-T. Leonardo and R.-R. Fábio, *Anal. Methods*, **7**, 4396 (2015).
3. B. S. Sazzad, M. A. Fazal, A.-A. Haseeb and H. H. Masjuki, *RSC Adv.*, **6**, 60244 (2016).
4. D. Singh, D. Sharma, S. L. Soni, S. Sharma and D. Kumari, *Fuel*, **253**, 60 (2019).
5. F. L. Adam, A. B. James, C. M. Jinesh and W. Karen, *Chem. Soc. Rev.*, **43**, 7887 (2014).
6. L. L. Ana, M. R. Célia and J.-M. Claudio, *Catal. Sci. Technol.*, **6**, 2877 (2016).
7. Z. Lillah, A. N. Toh and Z. Li, *Green Chem.*, **16**, 1202 (2014).
8. A. M. Juan, I. Jose and M. Gabriel, *Green Chem.*, **11**, 1285 (2009).
9. L. Pedro, M. B. Juana, G. V. Eduardo, S. G. Gregorio, V. Michel, M. I. Burguete and V. L. Santiago, *Green Chem.*, **17**, 3706 (2015).
10. G. K. Avinash, N. M. Prashant and R. B. Pundlik, *RSC Adv.*, **6**, 105087 (2016).
11. F. Su and Y. Guo, *Green Chem.*, **16**, 2934 (2014).
12. Z. Lillah, G. Tan and Z. Li, *Green Chem.*, **14**, 3077 (2012).

13. S. K. Naomi, H. Kousuke, I. Toru, N. Kazunori and Y. Toshikuni, *Fuel*, **139**, 11 (2015).
14. P. Liu, J. W. Hao, L. P. Mo and Z. H. Zhang, *RSC Adv.*, **5**, 48675 (2015).
15. P. Chantamanee, S. Noriaki, S. Nut, C. Tawatchai and T. Hajime, *Green Chem.*, **16**, 4936 (2014).
16. H. S. Siew, F. Y. Kian, T. L. Keat, S. Bhatia and H. T. Soon, *RSC Adv.*, **3**, 9070 (2013).
17. Q. Zhang, D.-V. Karine, R. Sébastien and J. François, *Chem. Soc. Rev.*, **41**, 7108 (2012).
18. F. Liu, D.-V. Karine, P. T. Marc, P. Yannick, J. M. Clacens, D. Floryan and J. François, *Green Chem.*, **15**, 901 (2013).
19. B. P. Sunanda and S. S. Ganapati, *Green Chem.*, **12**, 458 (2010).
20. T. N. Hai and H. T. Phuong, *RSC Adv.*, **6**, 98365 (2016).
21. J. Cao, B. Qi, J. Liu, Y. Shang, H. Liu, W. Wang, J. Lv, Z. Chen, H. Zhang and X. Zhou, *RSC Adv.*, **6**, 21612 (2016).
22. Y. R. Lee, Y. J. Lee, W. Ma and H. R. Kyung, *Korean J. Chem. Eng.*, **33**(8), 2337 (2016).
23. P. H. Tran and A.-T. Hang, *RSC Adv.*, **8**, 11127 (2018).
24. L. Gu, W. Huang, S. Tang, S. Tian and X. Zhang, *Chem. Eng. J.*, **259**, 647 (2015).
25. C. Swapnendu, B. Sourav and C. Rajat, *RSC Adv.*, **6**, 74278 (2016).
26. P. H. Michael, V. Amrit, L. C. Scott, L. C. Julie, W. L. Joseph, J. M. Eric and J. R. Aaron, *Phys. Chem. Chem. Phys.*, **19**, 28153 (2017).
27. T. Marek, T. Stefan, S. Vasil and N. Jacek, *Green Chem.*, **15**, 1615 (2013).
28. P. V. Sergey and H. Andreas, *J. Chem. Soc.*, **2**, 728 (2002).
29. A. Fredenslund and P. Rasmussen. *AIChE J.*, **25**(1), 203 (1979).
30. C. Reid and J. M. Prausnitz, *The properties of gases and liquids*, McGraw-Hill, New York (1987).
31. A. Fredenslund, L. J. Russell and J. M. Prausnitz, *AIChE J.*, **21**(6), 1086 (1975).
32. P. J. Barrie, *Phys. Chem. Chem. Phys.*, **14**, 318 (2012).